

NJC

Accepted Manuscript



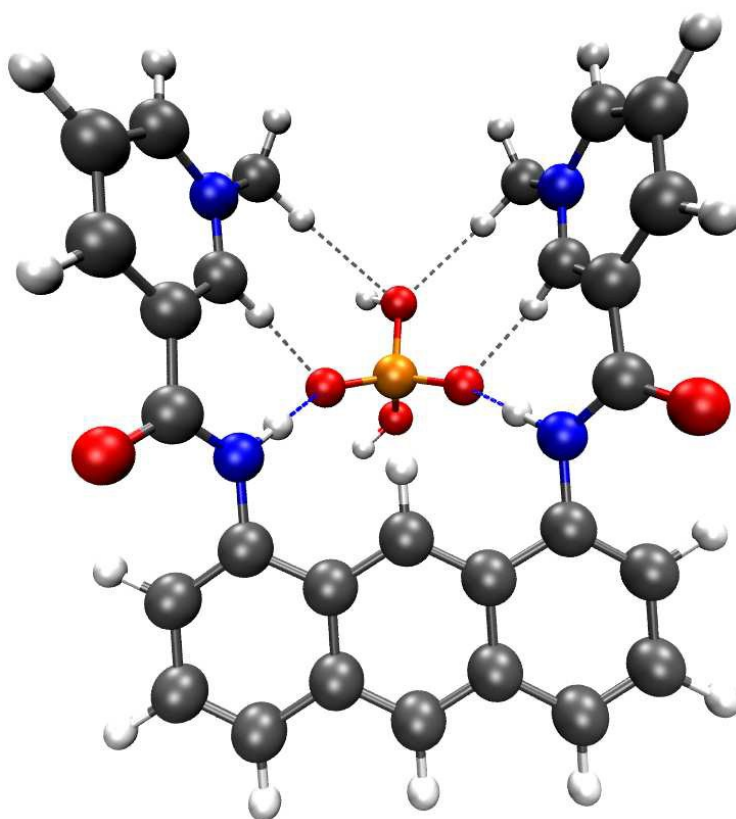
This is an *Accepted Manuscript*, which has been through the Royal Society of Chemistry peer review process and has been accepted for publication.

Accepted Manuscripts are published online shortly after acceptance, before technical editing, formatting and proof reading. Using this free service, authors can make their results available to the community, in citable form, before we publish the edited article. We will replace this *Accepted Manuscript* with the edited and formatted *Advance Article* as soon as it is available.

You can find more information about *Accepted Manuscripts* in the [Information for Authors](#).

Please note that technical editing may introduce minor changes to the text and/or graphics, which may alter content. The journal's standard [Terms & Conditions](#) and the [Ethical guidelines](#) still apply. In no event shall the Royal Society of Chemistry be held responsible for any errors or omissions in this *Accepted Manuscript* or any consequences arising from the use of any information it contains.

Graphical Abstract



Binding abilities depends on magnitude of C-H polarization.

Contribution of polar C-H Hydrogen Bonds on anion binding

Yusun Choi, Taehoon Kim, Soonmin Jang*, Jongmin Kang*

Department of Chemistry, Sejong University, Seoul, 143-747, South Korea

kangjm@sejong.ac.kr

Abstract

Contribution of C-H hydrogen bonds is one of the key factors to consider in anion binding receptor design. To investigate the participation of C-H hydrogen bonds through C-H polarization in the anion binding event, we have designed and synthesized three new anion receptors (receptor **1**, **2** and **3**). Essentially, the only difference within these receptors is the relative magnitude of C-H(H_a) polarization. These receptors utilize two amide N-H, two aromatic C-H(H_a), anthracene 9-C-H and possibly two methyl group as hydrogen bonding moieties. From the titrations and DFT calculations, we found that that the anion binding abilities of these receptors mainly depends on the magnitude polarization of C-H(H_a) and receptor **1** and **2** are selective for H₂PO₄⁻.

Key words : anion receptor, polar C-H hydrogen bonds

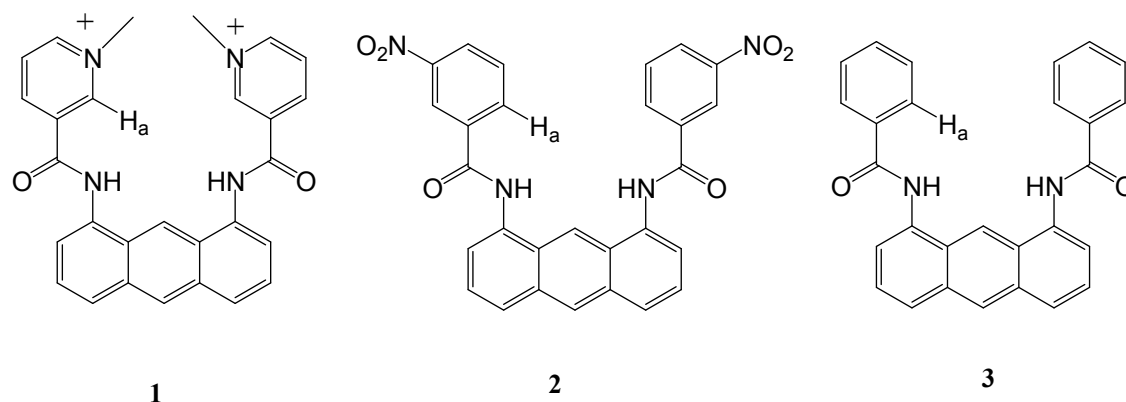
Introduction

The design and synthesis of efficient receptors capable of binding biologically and environmentally important anionic species is an emerging field in supramolecular chemistry.¹⁻

Hydrogen bonds are important anion recognition elements due to their directionality. As anions display a wide range of geometries, the directionality of hydrogen bonds is frequently utilized to achieve complementarity between anions and receptors. While most hydrogen bonding anion receptors utilize a N-H...anion or O-H...anion hydrogen bond, Only a few examples are reported about receptors utilizing C-H...anion hydrogen bonds⁶⁻¹³ even though C-H...anion hydrogen bonds play an important role in nature.¹⁴⁻²⁰ Although there have been many examples that C-H hydrogen bonds contribute to anion binding events, there appears to be a general consensus among supramolecular chemists that C-H hydrogen bonds are much weaker than traditional O-H and N-H donors.

However, when attached to polarizing substituents, C-H groups play as moderate-to strong hydrogen bond donors, exhibiting interaction energies comparable to those obtained from O-H and N-H groups.²¹⁻³²

To investigate the participation of C-H hydrogen bonds through C-H polarization in the anion binding event, we have designed and synthesized new anion receptors **1**, **2** and **3** as shown below



These receptors utilize two amide N-H, two aromatic C-H(H_a) and anthracene 9-C-H as hydrogen bonding moieties. From our experiments, we found that the binding abilities of

these receptors depends on the magnitude polarization of C-H_a. Here we report the synthesis and binding properties of these receptors.

Experimental section

Materials

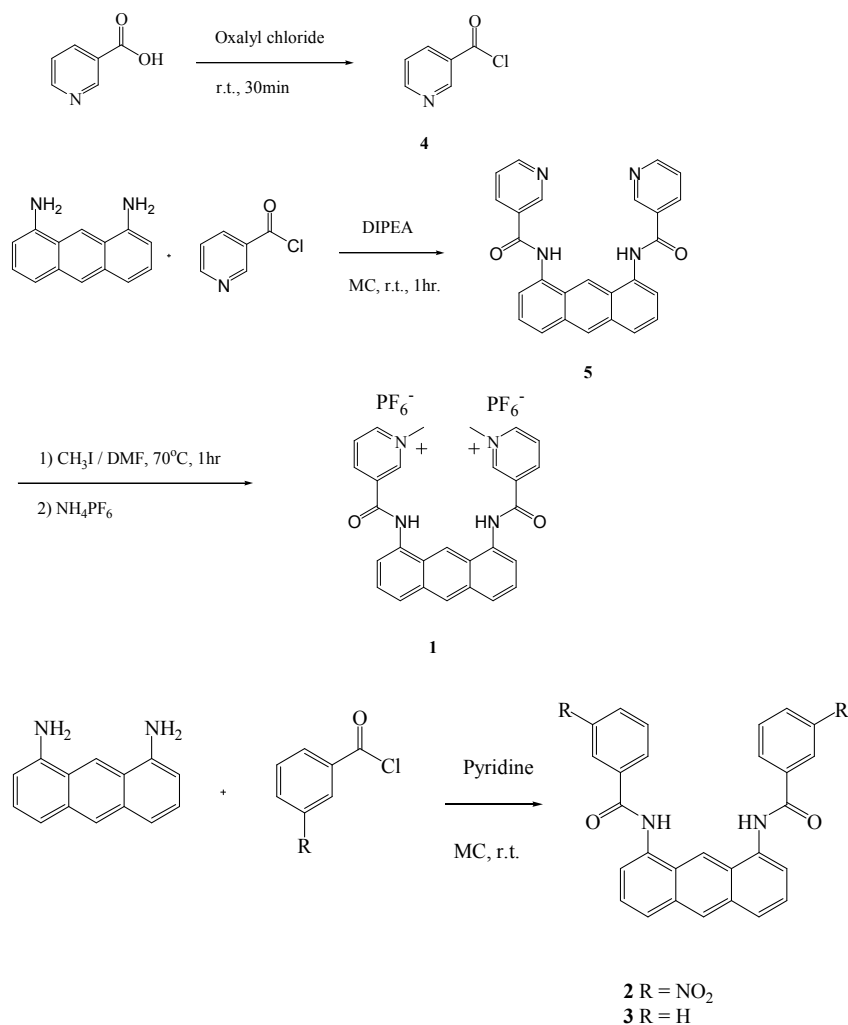
Tetra-n-butylammonium hydroxide, tetra-n-butylammonium fluoride, tetra-n-butylammonium dihydrogen phosphate, tetra-n-butylammonium acetate (TBAA), and tetranbutylammonium bromide, tetra-n-butylammonium chloride (TBACl) tetra-n-butylammonium hydrogen sulphate were purchased from Sigma-Aldrich Chemical Co., Inc., and used as received.

Measurements

Absorption spectra were recorded using a biochrom Libra S70 spectrophotometer (Biochrom Ltd, England). NMR spectra were recorded using a BRUKER spectrometer operated at 500 MHz. ESI MS spectra were obtained using a JMS 700 (Jeol, Japan) double focusing magnetic sector mass spectrometer. All measurements were carried out at room temperature (298 K).

Synthesis

For the synthesis of receptor **1**, nicotinic acid and oxalyl chloride was reacted to give nicotinoyl chloride **4** in quantitative yield. The reaction between nicotinoyl chloride and anthracene-1,8-diamine³³ in the presence of diisopropylethylamine gave N,N'-(anthracene-1,8-diyl)dinicotinamide **5** in 20% yield. Then compound **5** was reacted with 14 equivalents of methyl iodide at 70°C. Anion exchange with ammonium hexafluorophosphate gave receptor **1** in 72% yield. Receptors **2** and **3** were synthesized by the reaction between anthracene-1,8-diamine and 3-nitrobenzoyl chloride (or benzoyl chloride). All compounds were characterized by ¹H NMR, ¹³C NMR, and high-resolution mass spectrometry.

Scheme 1. Synthetic Procedure for Anion Receptors **1**, **2** and **3****Compound 4**

A suspension of 150 mg (1.22 mmol) of nicotinic acid in 1 ml of oxalyl chloride was stirred for 30 min at room temperature. After oxalyl chloride was evaporated in vacuo, the compound **4** was obtained in quantitative yield and used for next reaction without purification.

^1H NMR (CDCl_3 , 500MHz) δ 9.45(s, 1H), 9.06(d, 1H, $J=4.5\text{Hz}$), 8.91(d, 1H, $J=8\text{Hz}$), 8.05(t, 1H, $J=5.5\text{Hz}$)

Compound 5

To a solution of anthracene-1,8-diamine (127 mg, 0.61 mmol) in dichloromethane (7 mL) was added nicotinoyl chloride (173 mg, 1.22 mmol) and diisopropylethylamine (212 μL , 1.22 mmol) and stirred for 1 hour at room temperature. The precipitate was collected by filtration, washed with methanol and dried in vacuum to give dark brown solid (52 mg) in 20 % yield.

mp 264-268 $^\circ\text{C}$ ^1H NMR (DMSO-d_6 , 500MHz) 10.80(s,2H), 9.21(s, 2H), 8.91(s, 1H), 8.78(d, 2H, $J=4.5\text{Hz}$), 8.74(s, 1H), 8.36(d, 2H, $J=7.5\text{Hz}$), 8.08(d, 2H, $J=8.5\text{Hz}$), 7.75(d, 2H, $J=7\text{Hz}$), 7.66(t, 2H, $J=7.5\text{Hz}$), 7.48(m, 2H), ^{13}C NMR (DMSO-d_6 , 125MHz) δ 162.83, 146.25, 143.93, 142.39, 133.14, 132.45, 131.84, 126.95, 126.51, 126.33, 126.05, 125.58, 122.31, 118.18 HRMS(EI) m/z calcd for $\text{C}_{26}\text{H}_{18}\text{N}_4\text{O}_2$: 418.1430. Found : 418.1427.

Receptor 1

To a solution of $\text{N,N}'$ -(anthracene-1,8-diyl)dinicotinamide **5** (35mg, 0.084mmol) in DMF (3 mL) was added methyl iodide (73 μL , 1.18 mmol) and stirred for 1 hour at 70 $^\circ\text{C}$. After the reaction mixture was cooled to room temperature, 10 ml of water was added. Then, 5 ml of 1M NH_4PF_6 solution was added to give a dark brown precipitate. The precipitate was collected by filtration, washed with water and dried in vacuum to give dark brown solid (44.7 mg) in 72 % yield. mp > 300 $^\circ\text{C}$ ^1H NMR (DMSO-d_6 , 500MHz) δ 11.12(s,2H), 9.60(s, 2H), 9.15(m, 4H), 8.95(s, 1H), 8.81(s, 1H), 8.26(t, 2H, $J=6.5\text{Hz}$), 8.15(d, 2H, $J=8.5\text{Hz}$), 7.87(d, 2H, $J=7\text{Hz}$), 7.67(t, 2H, $J=7.5\text{Hz}$), 5.51(s, 6H) ^{13}C NMR (DMSO-d_6 , 125MHz) δ 161.48, 147.42,

146.11, 143.17, 133.86, 132.44, 131.83, 127.53, 127.16, 127.03, 126.38, 125.58, 122.77, 117.08, 48.27 HRMS (FAB), m/z calcd for $C_{28}H_{24}F_{12}O_2P_2$: 738.1183. Found: 738.1177.

Receptor 2

To a solution of anthracene-1,8-diamine (70 mg, 0.34 mmol) in dichloromethane (16 mL) was added 3-nitrobenzoyl chloride (125 mg, 0.68 mmol) and pyridine (127 μ l, 1.58 mmol) and stirred for 15 min. The precipitate was collected by filtration, washed with methanol and dried in vacuum to give light brown solid (110 mg) in 65 % yield. mp > 300°C 1H NMR (DMSO- d_6 , 500MHz) δ 10.92(s,2H), 8.76(m, 3H), 8.71(s, 1H), 8.35(m, 4H), 8.11(d, 2H, $J=7$ Hz), 7.62(m, 6H) ^{13}C NMR(DMSO- d_6 , 125MHz) δ 164.01, 147.51, 135.56, 133.88, 133.61, 131.85, 129.89, 129.89, 127.34, 126.98, 126.03, 125.46, 123.66, 122.21, 118.075 HRMS (FAB), m/z calcd for $C_{28}H_{18}N_4O_6 - H^+$:505.1146. Found: 505.1142

Receptor 3

To a solution of anthracene-1,8-diamine (60 mg, 0.29 mmol) in dichloromethane (9 mL) was added benzoyl chloride (80 mg, 0.57 mmol) and pyridine (109 μ l, 1.35 mmol) and stirred for 30 min. The precipitate was collected by filtration, washed with methanol and dried in vacuum to give black solid receptor **3** (70 mg) in 59 % yield. mp 274-276 °C 1H NMR (DMSO- d_6 , 500MHz) δ 10.59(s,2H), 8.92(s, 1H), 8.71(s, 1H), 8.04(m, 6H), 7.70(d, 2H, $J=6.5$ Hz), 7.59(q, 4H, $J=6.5$ Hz), 7.42(m, 4H) HRMS (FAB), m/z calcd for $C_{28}H_{19}N_2O_2 - H^+$:415.1445. Found : 415.1441

Results and Discussion

Interactions with Dihydrogen Phosphate

The ability of receptor **1** to recognize dihydrogen phosphate was studied first in DMSO using UV-vis titration spectra. Receptor **1** displayed absorption bands at 390 nm. Upon addition of increasing amounts of H_2PO_4^- , moderate increases in absorption at 455 nm and isosbestic point was observed at 386 nm, suggesting typical hydrogen bonding complex formation between receptor **1** and dihydrogen phosphate. (Figure 1a)

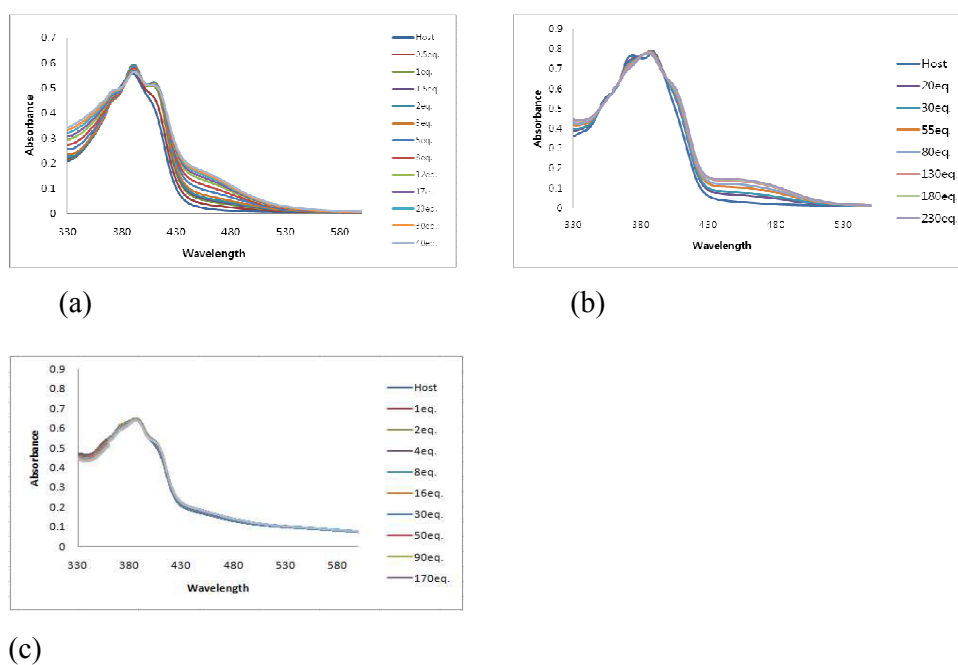
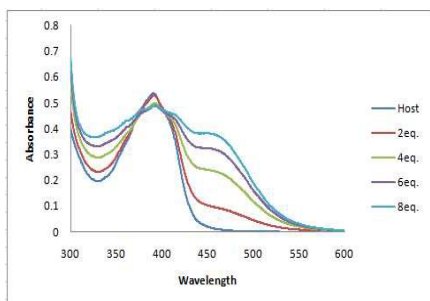


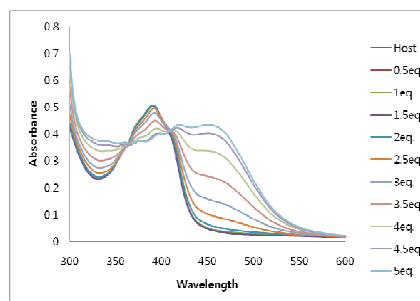
Figure 1. UV-vis spectra recorded over the course of titration of 100 μM DMSO solution of the receptor **1**(a), **2**(b) and **3**(c) with the standard solution tetrabutylammonium dihydrogen phosphate

In order to discriminate hydrogen bonding interaction from deprotonation, UV-vis titration of the receptor **1** with tetrabutylammonium hydroxide was carried out (Figure 2a). The changes in the absorbance spectra with hydroxide were clearly different from those with dihydrogen phosphate. Furthermore, isosbestic points observed at 406nm and 370 nm was different from the isosbestic points observed with dihydrogen phosphate. In addition, the UV-vis spectral

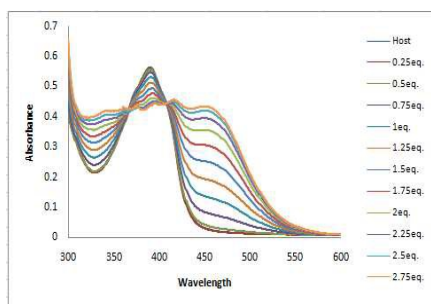
changes of the receptors upon addition of excessive fluoride or acetate were nearly identical to those triggered by hydroxide. (Figure 2b and 2c)



(a)



(b)



(c)

Figure 2. UV-vis spectra recorded over the course of titration of 100 μM DMSO solution of the receptor **1** with the standard solution tetrabutylammonium hydroxide (a), tetrabutylammonium fluoride (b) and tetrabutylammonium acetate (c)

Receptor **1** showed a strong fluorescence emission spectrum in DMSO as expected. The excitation wavelength was 381 nm and emission wavelengths were 442 nm. The intensity of the emission spectrum from 20 μM solution of receptor **1** gradually increased as the concentration of tetrabutylammonium dihydrogen phosphate salts was increased (1–35 equiv.), which also indicates the association between receptor **1** and dihydrogen phosphate (Figure. 3).

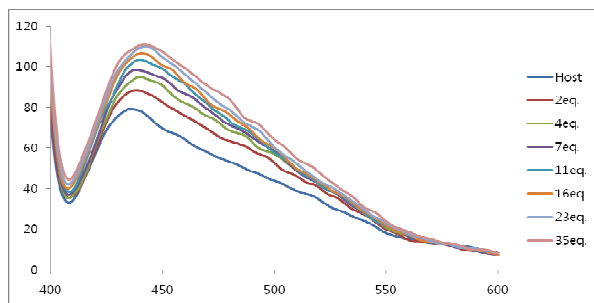


Figure. 3 The change in fluorescence spectra over the course of titration of 20 μ M DMSO solutions of receptor **1** when tetrabutylammonium dihydrogen phosphate was added. The change in the fluorescence of the intensity measured at 442 nm.

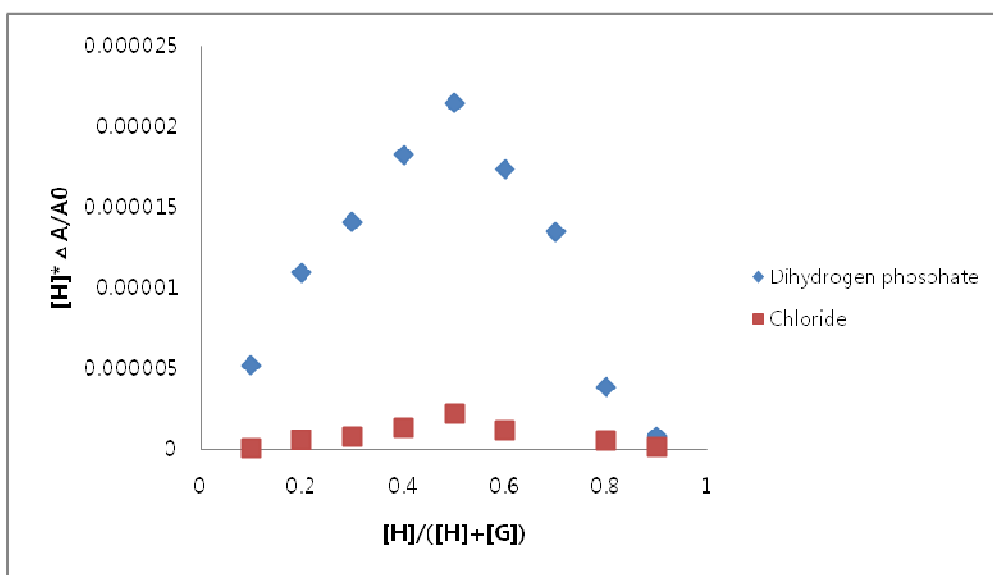


Figure 4. Job plots of receptor **1** with tetrabutylammonium dihydrogen phosphate and tetrabutylammonium chloride obtained by UV-vis spectrum in DMSO

The stoichiometry between receptor **1** and dihydrogen phosphate was determined to be 1:1 using a UV-vis Job plot in DMSO (Figure 4).

The complexation abilities of receptor **1** to dihydrogen phosphate was also measured by standard ^1H NMR titration experiments in DMSO- d_6 using a constant host concentration (2 mM) and increasing concentrations of dihydrogen phosphate. The addition of tetrabutylammonium dihydrogen phosphate salts to the solution of receptor **1** in DMSO- d_6 resulted in downfield shift

of C-H_a and anthracene 9-C-H peaks. For example, C-H_a peak moved from 9.602 ppm to 9.925 ppm and anthracene 9-C-H moved from 8.952 ppm to 9.473 ppm. However, no downfield shift of amide N-H peak was observed due to severe line broadening. (Figure 5) This result indicates that added dihydrogen phosphate are complexed by receptor **1** through amide N-H, C-H_a and anthracene 9-C-H. In addition, all peaks from anthracene showed upfield shift except 9-C-H peak. In fact, two effects are expected as a result of hydrogen bond formation between receptor **1** and the anion. (i) A through-bond propagation increases the electron density in the anthracene ring, which causes a shielding effect and promotes an upfield shift; (ii) a through-space effect increases a polarization of C-H bonds, which causes deshielding and promotes a downfield shift. In this case, the through-bond propagation dominates, and an upfield shift is observed for all hydrogen peaks from anthracene.

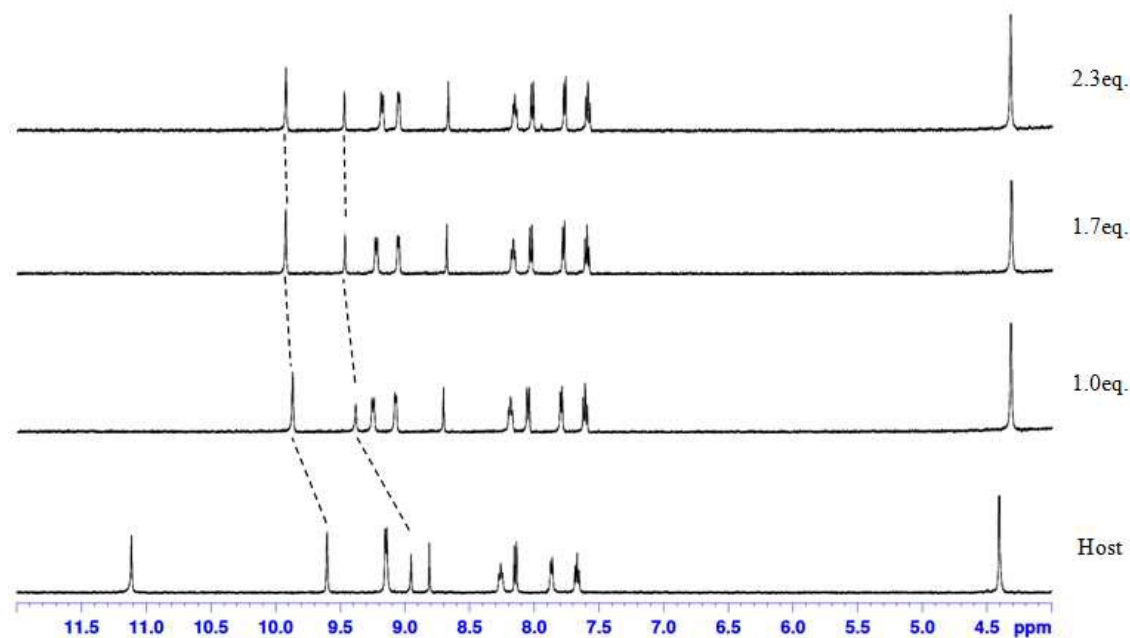


Figure 5. ¹H NMR spectra of 2 mM of receptor **1** containing increasing amounts of tetrabutylammonium dihydrogen phosphate (0 –2.3 equiv.) in DMSO-d₆

A Benesi–Hildebrand plot³⁴ by use of change at 455 nm in UV-vis spectrum and at 442 nm in fluorescence spectrum gave the association constant for dihydrogen phosphate. The calculated association constants for dihydrogen phosphate were 1.5×10^3 and 1.6×10^3 from UV-vis spectrum and fluorescence spectrum respectively. In addition, the chemical shifts of these hydrogens were analyzed by EQNMR³⁵ and the association constant calculated from ¹H NMR titration gave 1.3×10^3 , which is similar with the values obtained from UV-vis and fluorescence titrations.

In the case of receptor **2**, absorption bands appeared at 374, 388 nm in DMSO. Upon addition of increasing amounts of H_2PO_4^- , formation of hydrogen bonding complex was also observed. A new λ_{max} was observed at 447 nm and isosbestic point was observed at 399 nm. (Figure 1b) Receptor **2** also showed hydrogen bond formation through ¹H NMR titration. Until 8 equivalents of dihydrogen phosphate was added, amide N-H peak moved from 10.9 to 12.2 ppm although line broadening was observed. (Figure 6) In addition, downfield shifts of C-H_a peak (para position to NO₂ group) and anthracene 9-C-H were observed. For example, C-H_a peak moved from 8.35 ppm to 8.87 ppm and anthracene 9-C-H moved from 8.69 ppm to 9.06 ppm. This result indicates that these hydrogens are major hydrogens involved in hydrogen bonding with anions during titration and added dihydrogen phosphate are complexed by receptor **2** through amide N-H, C-H_a and anthracene 9-C-H. The calculated association constants between receptor **2** and dihydrogen phosphate were 2.1×10^2 from UV-vis titration and 2.2×10^2 from ¹H NMR.

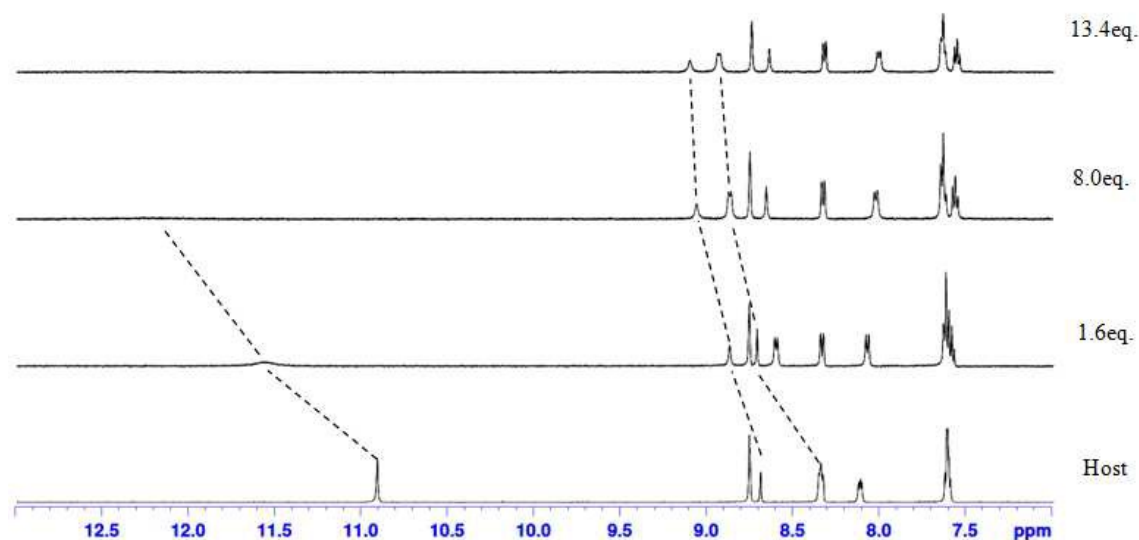
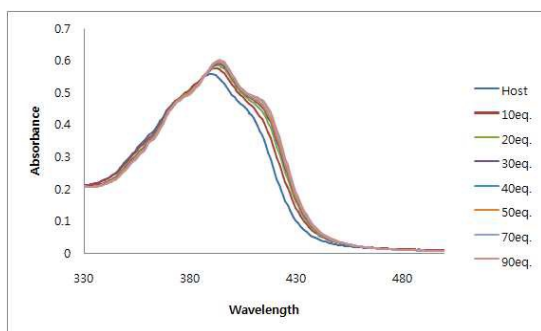


Figure 6. ^1H NMR spectra of 2 mM of receptor **2** containing increasing amounts of tetrabutylammonium dihydrogen phosphate (0 –13.4 equiv.) in DMSO-d_6

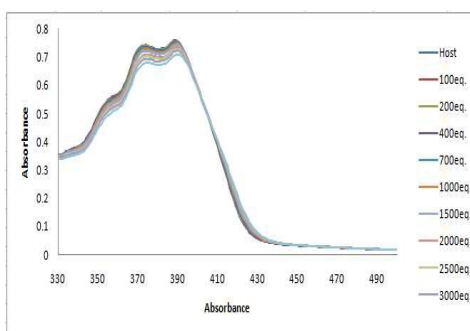
No change of spectrum was observed with receptor **3** (Figure 1c). Most likely two amide N-H hydrogen bonds, the polarization of anthracene 9-H and C-H_a are not strong enough to make complex with dihydrogen phosphate, which indicates the importance of polarization of C-H_a in the receptor **1** and **2**.

Interactions with halides

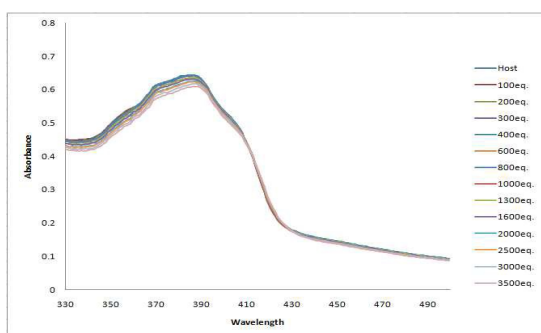
The abilities of receptor **1** to recognize halides were also studied in DMSO using UV–vis titration spectra. When the amount of chloride was increased, moderate decreases in absorbance below isosbestic point and moderate increases in absorbance above isosbestic point were observed (Figure 7a). Isosbestic point was observed at 387 nm, suggesting typical hydrogen bonding complex formation between receptor **1** and chloride. The existence of isosbestic point for UV-vis titrations of receptors **1** with chloride suggests a 1:1 complexation, and this was also confirmed by Job's plot analysis (Figure 4).



(a)



(b)



(c)

Figure 7. UV-vis spectra recorded over the course of titration of 100 μ M DMSO solution of the receptor **1**(a), **2**(b) and **3**(c) with the standard solution tetrabutylammonium chloride.

However, no changes of spectra due to chloride were observed with receptor **2** and **3**. (Figure 7b and 7c), which also indicates the importance of polarization of C-H_a in these receptors.

The formation of hydrogen bond between receptor **1** and chloride was clearly observed through ¹H NMR titration. Until 45 equivalents of chloride was added, amide N-H peak moved from 11.12 to 11.54 ppm. In addition, downfield shift of C-H_a peak and anthracene 9-C-H observed. For example, C-H_a peak moved from 9.60 ppm to 9.93 ppm and anthracene 9-C-H moved from 8.95 ppm to 9.54 ppm. The association constants calculated for chloride

were 7.1×10^2 . Bromide showed similar behaviors to chloride in UV-vis titration and ^1H NMR titration (see supporting information). The calculated binding constants for other anions are summarized in Table 1.

Anion	1		2	
	UV	NMR	UV	NMR
H_2PO_4^-	1.5×10^3	1.3×10^3	2.1×10^2	2.2×10^2
Cl^-	7.3×10^2	7.1×10^2	nb	nb
Br^-	1.6×10^2	1.6×10^2	nb	nb
HSO_4^-	7.0×10	3.5×10	nb	nb

Table 1. Association constants (M^{-1}) of receptors **1** and **2** with various anions in CH_3CN . Nb means no binding

Modeling studies.

To account for the binding affinity of anions, we have carried out a series of DFT electronic structure calculation of each receptor, two anions, i.e. H_2PO_4^- and Cl^- , and their complexes. We prepared the initial geometry of each compound with Spartan'10³⁶ and performed systematic conformational search with DFT calculation by changing the dihedral angles of the receptors with Gaussian09 package³⁷. In this stage, we also included three low energy conformers obtained from simulated annealing, using molecular mechanics force field (MMFF) as implemented in Spartan'10, followed by DFT optimization calculation. As for the complex, we placed the anions on the DFT optimized receptors and performed separate DFT optimization by changing the location/orientation of anion relative to the receptor. All DFT calculations were done with B3LYP/6-311+G(d,p) level under the polarizable continuum model (PCM) using DMSO as solvent as implemented in Gaussian09 package. Basically, the receptors do not have a significant amount structural flexibility due to the

highly conjugated nature with the exception of several diheadral angles. Therefore, we believe the current scheme is more than sufficient enough for searching the lowest energy conformer in this study. During the DFT calculations, we have not imposed symmetry conditions. The binding energies of each receptor with H_2PO_4^- and Cl^- anions are obtained from the DFT energy difference between the complex and the receptor + anion. For all six cases, three receptors in combination with two anions, the complex energy is lower than the combined energy of the receptor and the anion alone. The final structures of receptor **1** in complex with anions are shown in Figure 8. The complex structures of the other two receptors are essentially the same and are therefore not shown here. All figures are drawn with Pymol³⁸.

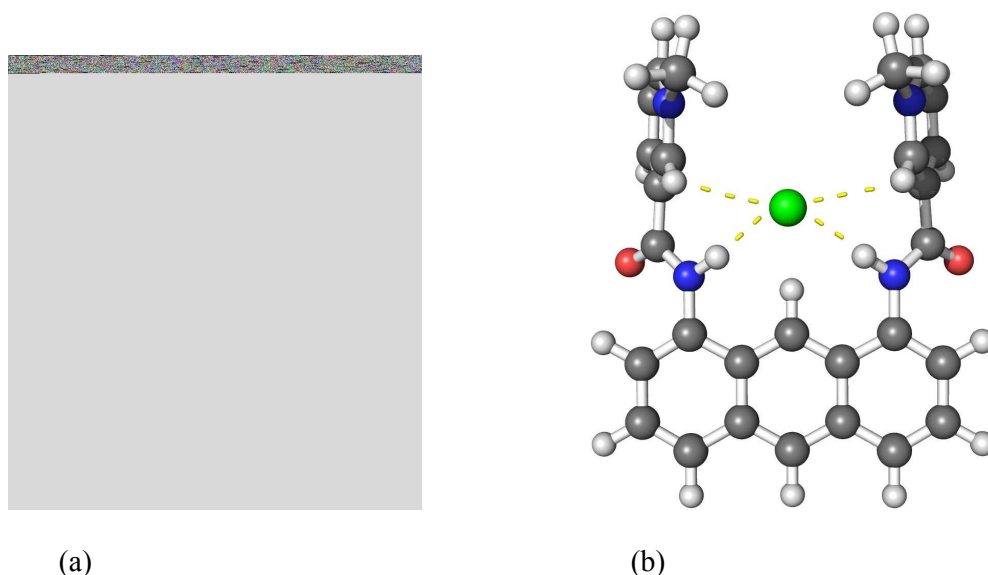


Figure 8. Receptor **1** in complex with H_2PO_4^- (a) and Cl^- .

One can immediately notice that the H_2PO_4^- anions are making complex with receptors by hydrogen bonds between two non-hydrogen connected oxygen atoms on H_2PO_4^- and amide hydrogens and aromatic hydrogens (C-H_a) on the receptor.

The binding energies, obtained from energy difference as state above, of each receptor with both anions are listed in Table 2.

	Receptor 1	Receptor 2	Receptor 3
H ₂ PO ₄ ⁻	-29.45	-18.48	-16.63
Cl ⁻	-12.13	-5.10	-3.17

Table 2. The binding energies of three complexes with two anions. Units are in kcal/mol.

The binding energy table shows receptor 1 is the most capable receptors for both H₂PO₄⁻ and Cl⁻ anions among three receptors and receptor 2 and 3 has similar binding affinity. For all receptors the binding affinity with H₂PO₄⁻ anion is higher than Cl⁻ anion. All these results are in agreement with experiment at least qualitatively.

We are particularly interested on the partial charges on C-H_α hydrogen and hydrogen on amide N-H. The partial charges of these hydrogens, before and after complex formation, obtained from Mulliken population analysis are listed on Table 3.

	Receptor 1			Receptor 2			Receptor 3		
	No anion	H ₂ PO ₄ ⁻	Cl ⁻	No anion	H ₂ PO ₄ ⁻	Cl ⁻	No anion	H ₂ PO ₄ ⁻	Cl ⁻
C-H _α	0.189	0.213 (0.218)	0.199	0.138	0.168	0.148	0.116	0.136 (0.150)	0.136
N-H	0.263	0.328 (0.321)	0.281	0.256	0.316 (0.314)	0.269	0.253	0.317	0.270

Table 3. The hydrogen partial charges in electron unit on C-H_α and amide N-H for each receptor before and after the binding with anions. The values in parenthesis, if present, indicate charges on the other side of receptor.

We also listed the bond distances involved in hydrogen bonds in Table 4

	Receptor 1		Receptor 2		Receptor 3	
	H ₂ PO ₄ ⁻	Cl ⁻	H ₂ PO ₄ ⁻	Cl ⁻	H ₂ PO ₄ ⁻	Cl ⁻
C-H _a	1.9785 (1.9593)	2.7466	2.1016 (2.1013)	2.5922 (2.5916)	2.1981 (2.1901)	2.6816
N-H	1.7689 (1.7870)	2.4441	1.8030 (1.7971)	2.6038 (2.6044)	1.8118 (1.8163)	2.6332

Table 4. The bond distances involved in complex formation. The values in parenthesis, if present, indicate distance on the other side of receptor. Units are in Å.

Consistent with the binding energy trend, receptor **1** has the shortest hydrogen bond distances between receptor and anion while the distances are comparable between receptor **2** and receptor **3**. Both from the charge table and hydrogen bond distance table, it is clear that both hydrogens on C-H_a and amide N-H of receptor **1** have highly positive charge compare to two other receptors, indicating that compound **1** is the more efficient anion receptor, supporting our experimental results. Based on these calculations, the enhanced anion binding affinity of receptor **1** is attributed not only to the hydrogen partial charge on C-H_a, but also the increased positive charge on amide hydrogens. We also noted that there are very weak charge-charge interaction between hydrogen atoms on methyl group and one of the hydrogen bound oxygen atom in H₂PO₄⁻ anion for receptor **1**. Their distance is about 2.5 Å and this might have played an extra role in the complex of receptor **1** with H₂PO₄⁻ anion.

Conclusion

The contribution of C-H hydrogen bonds through C-H polarization was demonstrated through

three new anion receptors **1**, **2** and **3**. These receptors utilize two amide N-H, two aromatic C-H(H_a), anthracene 9-C-H and possibly two methyl group as hydrogen bonding moieties and only the relative magnitude of C-H(H_a) polarization makes differences in the anion binding events among these receptors. From the titration and DFT calculation, we found that that binding abilities of these receptors mainly depends on the magnitude polarization, or charge separation of C-H(H_a) and receptor **1** and **2** are selective for $H_2PO_4^-$.

Acknowledgments

This research was supported by the Basic Science Research Program of the Korean National Research Foundation funded by the Korean Ministry of Education, Science and Technology (2010-0021333). SJ acknowledges financial support from Korean National Research Foundation (2012R1A1A2009242).

References

1. P. de Hoog, P. Gamez, I. Mutikainen, U. Turpeinen, J. Reedijk, *Angew. Chem.* 2004, **116**, 5939 – 5941
2. J. L. Sessler, D. Seidel, *Angew. Chem.* 2003, **115**, 5292 – 5333
3. P. D. Beer, P. A. Gale, *Angew. Chem.* 2001, **113**, 502 – 532
4. J. Y. Kwon, N. J. Singh, H. N. Kim, S. K. Kim, K. S. Kim, J. Yoon, *J. Am. Chem. Soc.* 2004, **126**, 8892 – 8893
5. F. P. Schmidtchen, M. Berger, *Chem. Rev.* 1997, **97**, 1609 – 1646.
6. D.-W. Yoon, H. C.-H. Lee, *Angew. Chem. Int. Ed.* 2002, **41**, 1757-1759
7. W. S. Jonathan *Chem. Commun.* 2006, 2637–2649
8. K. Ghosh, G. Masanta, *Tetrahedron lett.* 2008, **49**, 2592-2597

9. H. F. Maria, D. Terry, D. Humphries, R. T. David, K. Ritu, K. Jaanus, W.S. Jonathan, *Chem. Commun.* 2006, 156–158
10. J. Cai, J. L. Sessler, *Chem. Soc. Rev.* 2014, **43**, 6198-6213
11. N. H. Evans, P. D. Beer, *Ang. Chem. Int. Ed. Engl.* 2014, **53**, 11716-11754
12. L. M. Hancock, E. Marchi, P. Ceroni, P. D. Beer, *Chem. Eur. J.* 2012, **18**, 11277-11283
13. N. G. White, P. D. Beer, *Chem. Commun.* 2012, **48**, 8499-8501.
14. S. Metzger, B. Lippert, *J. Am. Chem. Soc.* 1996, **118**, 12467 -12468
15. P. Auffinger, S. Louise-May, E. Westof, *J. Am. Chem. Soc.* 1996, **118**, 1181 -1189
16. G. R. Desiraju, *Acc. Chem. Res.* 1991, **24**, 290 – 296
17. T. Steiner, W. Saenger, *J. Am. Chem. Soc.* 1992, **114**, 10146 – 10154
18. C. V. K. Sharma, G. R. Desiraju, *J. Chem. Soc., Perkin Trans. 2* 1994, 2345 – 2352
19. T. Steiner, *J. Chem. Soc., Perkin Trans. 2* 1995, 1315 – 1319
20. J. D. Chaney, C. R. Goss, K. Folting, B. D. Santarsiero, M. D. Hollingworth, *J. Am. Chem. Soc.* 1996, **118**, 9432 – 9433.
21. S. In, S. J. Cho, K. H. Lee, J. Kang, *Org. Lett.* 2005, **7**, 3993-3996
22. S. K. Kim,; N. J. Singh, S. J. Kim, H. G. Kim, J. K. Kim, J. W. Lee, K. S. Kim, J. Yoon, *Org. Lett.* 2003, **5**, 2083-2086
23. S. Yun, H. Ihm, H. G. Kim, C.-W. Lee, B. Indrajit, K. S. Oh, Y. J. Gong, J. W. Lee, J. Yoon, H. C. Lee, K. S. Kim, *J. Org. Chem.* 2003, **68**, 2467-2470
24. H. Ihm, S. Yun, H. G. Kim, J. K. Kim, K. S. Kim, *Org. Lett.* 2002, **4**, 2897-2900
25. K. Sato, S. Arai, T. Yamagishi, *Tetrahedron Lett.* 1999, **40**, 5219-5222
26. F. Garcia, M. R. Torres, E. Matesanz, L. Sanchez, *Chem. Commun.* 2011, **47**, 5016–5018
27. V. Amendola, L. Fabbri, E. Monzani, *Chem. Eur. J.* 2004, **10**, 76 – 82

28. S.-I. Kondo, *Supramolecular Chemistry*. 2011, **23**, 29–36
29. R. O. Ramabhadran, Y. Hua, Y.-J. Li, A.-H. Flood, K. Raghavachari, *Chem. Eur. J.* 2011, **17**, 9123 – 9129
30. S. K. Dey, B.Ojha, G. Das, *CrystEngComm*. 2011, **13**, 269–278
31. Y. Li, Flood, H. Amar *Angew. Chem. Int. Ed.* 2008, **47**, 2649 –2652
32. Y. Hua, R. O. Ramabhadran, E. O. Uduehi, J. K. Karty, K. Raghavachari, A. H. Flood, *Chem. Eur. J.* 2011, **17**, 312 – 321.
33. J. L. Sessler, T. D. Mody, D. A. Ford, V. Lynch, *Angew. Chem. Int. Ed.* 1992, **31**, 452-455.
34. H. Benesi, H. Hildebrand. *J. Am. Chem. Soc.* 1949, **71**, 2703-2707.
35. Hynes, M.J. *J. Chem. Soc. Dalton Trans.* 1993, 311–312.
36. Spartan'10 Wave function, Inc. Irvine, CA, USA.
37. Gaussian 09, Revision C.01, M. J. Frisch, G. W. Trucks, H. B. Schlegel, G. E. Scuseria, M. A. Robb, J. R. Cheeseman, G. Scalmani, V. Barone, B. Mennucci, G. A. Petersson, H. Nakatsuji, M. Caricato, X. Li, H. P. Hratchian, A. F. Izmaylov, J. Bloino, G. Zheng, J. L. Sonnenberg, M. Hada, M. Ehara, K. Toyota, R. Fukuda, J. Hasegawa, M. Ishida, T. Nakajima, Y. Honda, O. Kitao, H. Nakai, T. Vreven, J. A. Montgomery, Jr., J. E. Peralta, F. Ogliaro, M. Bearpark, J. J. Heyd, E. Brothers, K. N. Kudin, V. N. Staroverov, R. Kobayashi, J. Normand, K. Raghavachari, A. Rendell, J. C. Burant, S. S. Iyengar, J. Tomasi, M. Cossi, N. Rega, J. M. Millam, M. Klene, J. E. Knox, J. B. Cross, V. Bakken, C. Adamo, J. Jaramillo, R. Gomperts, R. E. Stratmann, O. Yazyev, A. J. Austin, R. Cammi, C. Pomelli, J. W. Ochterski, R. L. Martin, K. Morokuma, V. G. Zakrzewski, G. A. Voth, P. Salvador, J. J. Dannenberg, S. Dapprich, A. D. Daniels, O. Farkas, J. B. Foresman, J. V. Ortiz, J. Cioslowski, and D. J. Fox, Gaussian, Inc., Wallingford CT, 2009.

38. The PyMOL Molecular Graphics System, Version 1.7.4 Schrödinger, LLC.